

Internal Cation Mobilities in the Molten Systems (Li-Rb)NO₃ and (Li-Cs)NO₃

Isao Okada and Ryuzo Takagi

Department of Electronic Chemistry, Tokyo Institute of Technology,
Nagatsuta, Midori-ku, Yokohama 227, Japan

and Kazutaka Kawamura

Research Laboratory for Nuclear Reactors, Tokyo Institute of Technology,
O-okayama, Meguro-ku, Tokyo, Japan

Z. Naturforsch. **34a**, 498–503 (1979); received February 16, 1979

The relative differences in internal cation mobilities are measured for the molten systems (Li-Rb)NO₃ and (Li-Cs)NO₃ over a wide range of temperatures and concentrations with a countercurrent electromigration method, and the internal mobilities are calculated from these results and the available data on the electrical conductivity.

The following phenomena are observed: (a) under some conditions the electrical mobility of Li⁺ is lower than that of the larger cation, (b) at a given temperature the mobility of Li⁺ decreases with increasing molar volume of the mixture, and (c) at low temperatures the isotherms of the mobility of the large cation show a maximum at some low concentration of that ion. These phenomena are interpreted in terms of the free space and the pair potential between cation and anion.

Introduction

In binary molten salt mixtures (Li-M)X it has been observed that under some conditions Li⁺ migrates more slowly than the larger cation M⁺ (MX = NaBr [11], NaNO₃ [2, 3], KCl [4, 5], KBr [1, 6–8], KNO₃ [2, 9], K₂SO₄ [10], CsCl [5], AgNO₃ [11–13], and TiNO₃ [14]). We shall name this kind of phenomenon the Chemla effect after Chemla, who discovered it [15]. Interpretations have been based on complex or the associated ion formation [6, 16, 17] and anion polarization [4]. Molecular dynamics simulations of the molten systems (Li-K)Cl and (Li-Rb)Cl did show, however, that the phenomenon could be interpreted in a different way [18]: the predominant factors ruling electrical conductivity seem to be ionic sizes in comparison with free space in the melt.

In a previous study on the system (Li-Tl)NO₃ [14] it has been observed that the isotherm of the mobility for Tl⁺ decreases drastically at low concentrations of TiNO₃, particularly at low temperatures. This can also be interpreted in terms of the ionic size as compared with the free space. This phenomenon had not been observed distinctly for other binary systems, probably because the larger

cations were not as large as Tl⁺ and also because the isotherms were examined at relatively high temperatures. Presumably because of the latter reason this phenomenon has not been found in a recent study on the system (Li-Cs)Cl [5], although Cs⁺ is larger than Tl⁺.

In the present study we have chosen Rb⁺ and Cs⁺ as the larger cations in order to clarify further the effect of ionic size on the mobility. Nitrate systems are chosen, because the relative difference in internal mobilities of the two cations, ϵ , can be measured more easily and accurately in them than in other systems such as chlorides. The quantity ϵ is measured with a countercurrent electromigration method (Klemm's method) and the internal cation mobilities are calculated from the ϵ values and the available data on the equivalent conductivity of these systems.

Experimental

The electromigration cell used is shown in Figure 1. This kind of cell was devised originally for the purpose of enriching ⁶Li [19]. Since metals do not electrodeposit at the cathode owing to electrolysis of NH₄⁺, it was not necessary to lead a mixture of NO₂ and O₂ into the cathode compartment, which was the usual practice in this kind of experiments. The upper part, containing molten NH₄NO₃, was kept at about 180 °C with an electric heater, and with another one the lower part was kept at the

Reprint requests to Dr. Isao Okada. Please order a reprint rather than making your own copy.

0340-4811 / 79 / 0400-0498 \$ 01.00/0



Dieses Werk wurde im Jahr 2013 vom Verlag Zeitschrift für Naturforschung in Zusammenarbeit mit der Max-Planck-Gesellschaft zur Förderung der Wissenschaften e.V. digitalisiert und unter folgender Lizenz veröffentlicht: Creative Commons Namensnennung-Keine Bearbeitung 3.0 Deutschland Lizenz.

Zum 01.01.2015 ist eine Anpassung der Lizenzbedingungen (Entfall der Creative Commons Lizenzbedingung „Keine Bearbeitung“) beabsichtigt, um eine Nachnutzung auch im Rahmen zukünftiger wissenschaftlicher Nutzungsformen zu ermöglichen.

This work has been digitalized and published in 2013 by Verlag Zeitschrift für Naturforschung in cooperation with the Max Planck Society for the Advancement of Science under a Creative Commons Attribution-NoDerivs 3.0 Germany License.

On 01.01.2015 it is planned to change the License Conditions (the removal of the Creative Commons License condition “no derivative works”). This is to allow reuse in the area of future scientific usage.

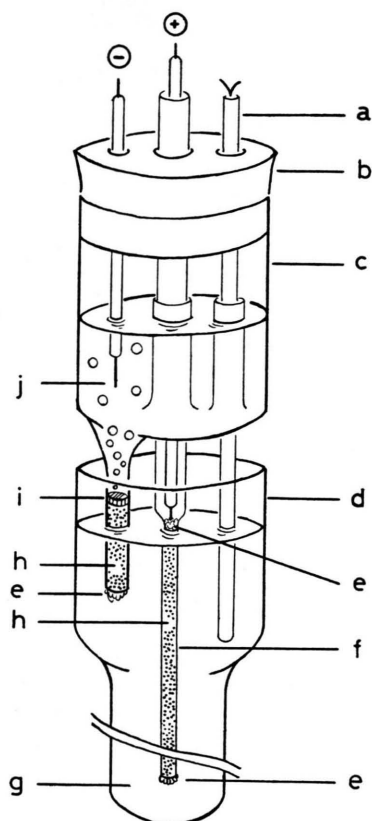


Fig. 1. Electromigration cell. a: thermocouple, b: silicone stopper, c: cathode compartment (quartz), d: quartz cell, e: quartz wool, f: separation tube (Vycor, int. diam.: 4 mm), g: molten (Li-Na-K)NO₃, h: quartz or alumina powder (80–100 mesh), i: quartz frit, j: molten NH₄NO₃. Quartz and alumina powders were used for the systems (Li-Rb)NO₃ and (Li-Cs)NO₃, respectively.

chosen temperature. A ternary mixture of (Li-Na-K)NO₃ with the eutectic composition was employed as the melt in the lower large compartment. Before electromigration, the mixture under investigation was held just below the melting points in vacuo for about 3 hr, then melting, dried argon gas being bubbled through it for about 1 hr, and then introduced into the separation tube. The choice of the lowest temperature for electromigration was based on the phase diagram of the mixtures ((Li-Rb)NO₃ [20] and (Li-Cs)NO₃ [21]). After electromigration, the content of cations in the separation tube was determined with flame spectrophotometry (Li) and atomic absorption spectrophotometry (Rb and Cs). Other experimental procedures were similar to those described previously [14].

Results

The quantity ε_{12} is defined by

$$\varepsilon_{12} = (b_1 - b_2) / \bar{b}, \quad (1)$$

where $b_{1,2}$ is the internal cation mobility, i. e. the cation mobility relative to the anion, and \bar{b} the averaged one, which is related to the equivalent conductivity, Λ , by

$$\bar{b} = p_1 b_1 + p_2 b_2 = \Lambda / F, \quad (2)$$

where p is the initial equivalent fraction of the corresponding cation and F Faraday's constant; the

Table 1. Conditions and results for the system (Li-Rb)NO₃. T was controlled within ± 3 K in most experiments. Q is the transported charge.

Run	T/K	p_{Rb}	Q/C	ε_{12}
1	570	0.859 ± 0.002	2270	-0.074 ± 0.002
2	645		2970	-0.128 ± 0.003
3	490		3410	0.021 ± 0.003
4	508	0.735 ± 0.010	2690	0.005 ± 0.003
5	531		1276	-0.031 ± 0.002
6	580		1908	-0.072 ± 0.004
7	601	0.575 ± 0.012	2855	-0.093 ± 0.007
8	639		2460	-0.123 ± 0.007
9	479		2592	0.088 ± 0.003
10	556	0.398 ± 0.003	2873	-0.013 ± 0.002
11	603		2777	-0.066 ± 0.004
12	653		3214	-0.099 ± 0.005
13	528	0.349 ± 0.012	1906	0.070 ± 0.003
14	588		2477	0.020 ± 0.003
15	629		1859	-0.009 ± 0.002
16	500	0.313 ± 0.003	2048	0.098 ± 0.004
17	514		3051	0.085 ± 0.003
18	568		3112	0.038 ± 0.003
19	329	0.260 ± 0.005	2843	0.023 ± 0.007
20	476		2785	0.103 ± 0.003
21	639		1570	0.009 ± 0.006
22	524	0.213 ± 0.005	2653	0.050 ± 0.002
23	574		2628	0.035 ± 0.002
24	628		3028	-0.004 ± 0.004
25	536	0.196 ± 0.003	3171	0.053 ± 0.002
26	561		3123	0.035 ± 0.003
27	576		3222	0.022 ± 0.002
28	624	0.065 ± 0.002	1906	0.000 ± 0.007
29	532		2623	0.057 ± 0.003
30	558		2027	0.040 ± 0.006
31	608	0.022 ± 0.000	2742	0.001 ± 0.003
32	626		2798	-0.008 ± 0.005
33	544		2623	0.135 ± 0.008
34	571		2974	0.103 ± 0.003
35	613		2212	0.073 ± 0.005
36	573		3101	0.236 ± 0.013
37	594		2352	0.111 ± 0.004
38	631		2211	0.100 ± 0.007

Table 2. Conditions and results for the system (Li-Cs)NO₃. *T* was controlled within ± 1 K in most experiments. *Q* is the transported charge.

Run	<i>T</i> /K	<i>p</i> Cs	<i>Q</i> / <i>C</i>	ε_{12}
101	638	0.899 \pm 0.001	1793	-0.279 \pm 0.043
102	660		1838	-0.304 \pm 0.009
103	575	0.735 \pm 0.002	1445	-0.130 \pm 0.019
104	593		1256	-0.123 \pm 0.007
105	606		1454	-0.133 \pm 0.006
106	608		1879	-0.143 \pm 0.009
107	669		2064	-0.161 \pm 0.006
108	524	0.567 \pm 0.003	2103	-0.018 \pm 0.006
109	531		2390	-0.023 \pm 0.007
110	559		2133	-0.051 \pm 0.017
111	593		1829	-0.082 \pm 0.016
112	658		1718	-0.096 \pm 0.011
113	686		1440	-0.111 \pm 0.007
114	553	0.338 \pm 0.002	1377	0.114 \pm 0.025
115	579		1610	0.065 \pm 0.005
116	633		1254	0.033 \pm 0.008
117	691		1672	-0.002 \pm 0.008
118	534	0.210 \pm 0.008	2240	0.151 \pm 0.010
119	557		2175	0.139 \pm 0.006
120	568		1458	0.138 \pm 0.011
121	609		2337	0.112 \pm 0.006
122	644		2052	0.076 \pm 0.003
123	658		1975	0.073 \pm 0.004
124	561	0.109 \pm 0.009	1428	0.189 \pm 0.015
125	589		2209	0.181 \pm 0.010
126	622		2077	0.139 \pm 0.006
127	653		2500	0.120 \pm 0.010
128	536	0.058 \pm 0.001	1384	0.554 \pm 0.030
129	561		1420	0.251 \pm 0.013
130	590		1863	0.199 \pm 0.008
131	637		1837	0.173 \pm 0.008

subscripts 1 and 2 stand for Li⁺ and the larger cation, i. e. Rb⁺ or Cs⁺, respectively.

The value of ε_{12} can be calculated from chemical analysis of the cations and the transported charge by use of an equation based on the material balance [10, 14]. Experimental conditions and the results are tabulated in Tables 1 and 2. The values of ε_{12} are plotted against temperature in Figs. 2 and 3 for the system (Li-Rb)NO₃ and in Fig. 4 for (Li-Rb)NO₃.

From Eqs. (1) and (2) it follows that

$$b_1 = (\Delta/F) (1 + p_2 \varepsilon_{12}), \quad (3a)$$

$$b_2 = (\Delta/F) (1 - p_1 \varepsilon_{12}). \quad (3b)$$

Isotherms of b_1 and b_2 are shown in Fig. 5 for the former system at 573 and 623 K, and in Fig. 6 for the latter at 543 and 643 K. The equivalent conductivities are calculated from the available data on specific conductivities ((Li-Rb)NO₃ [20] and (Li-Cs)NO₃ [22]) and densities [23].

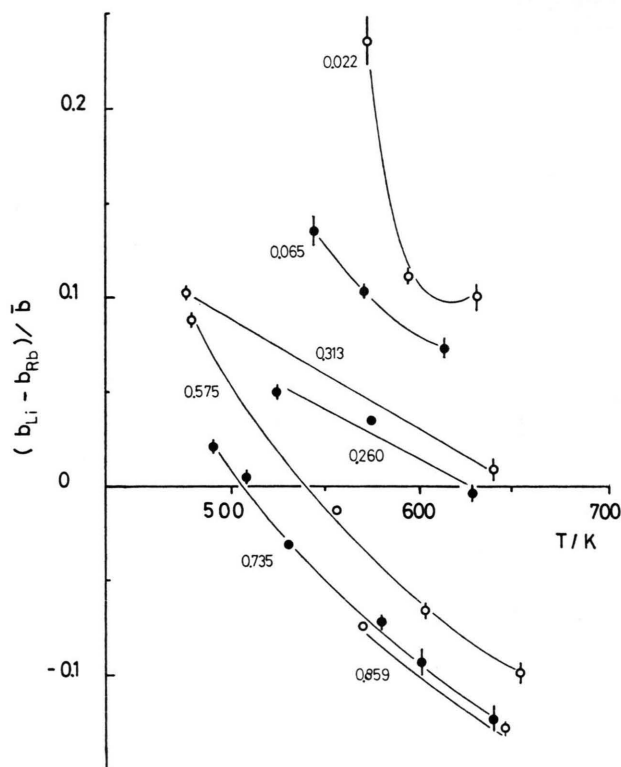


Fig. 2. Relative difference in internal cation mobilities against temperature in the system (Li-Rb)NO₃. The numbers in the figure represent the mole fraction of RbNO₃.

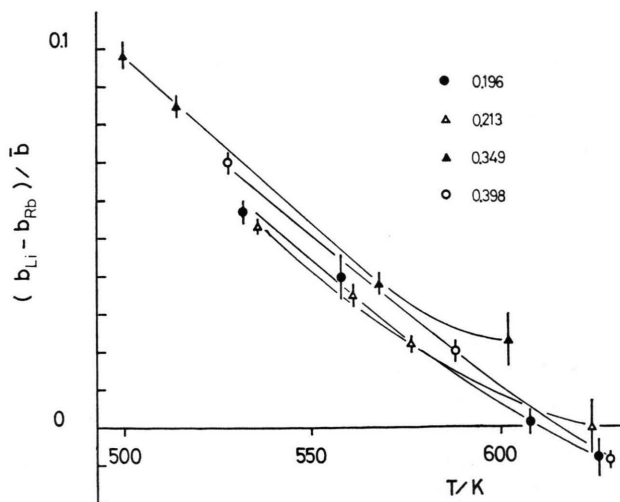


Fig. 3. Relative difference in internal cation mobilities against temperature in the system (Li-Rb)NO₃. See also legend of Figure 2.

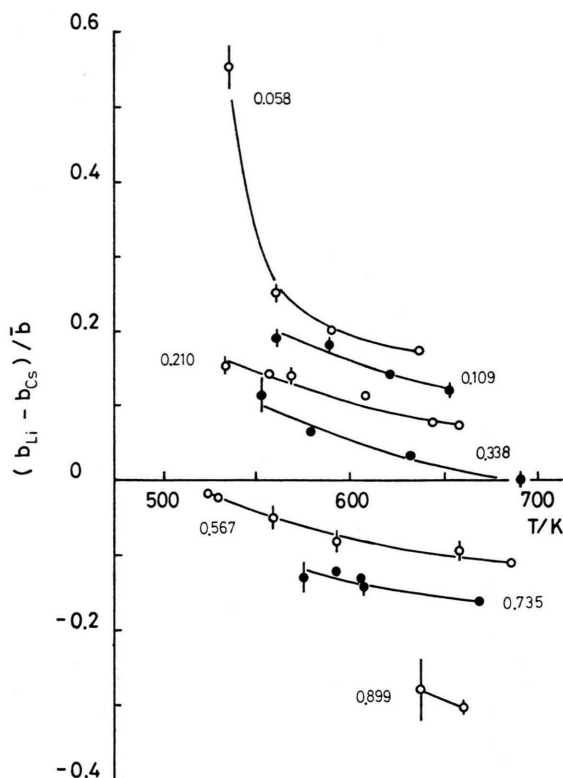


Fig. 4. Relative difference in internal cation mobilities against temperature in the system $(\text{Li-Cs})\text{NO}_3$. The numbers in the figure represent the mole fraction of CsNO_3 .

Discussion

The Chemla effect is observed in both $(\text{Li-Rb})\text{NO}_3$ and $(\text{Li-Cs})\text{NO}_3$, as shown in Figs. 5 and 6, respectively. In the former the isotherms of the two cation mobilities at relatively high temperatures cross each other at three points. Crossing at three points has not been found in any other systems so far and cannot be explained clearly at present.

Ionic mobilities can be expressed in terms of correlation functions between mean ionic velocities [24, 25]. This could be roughly approximated by the simplifying assumption that ionic mobilities would be related with a separating motion of the nearest neighbouring cations and anions. This assumption has been verified numerically for some alkali chlorides with molecular dynamics simulations [18]. Thus it is expected that, whereas the diffusion coefficient of Li^+ should be larger than that of a larger and heavier cation in molten mixtures, the mobility of the former would not always be higher than that

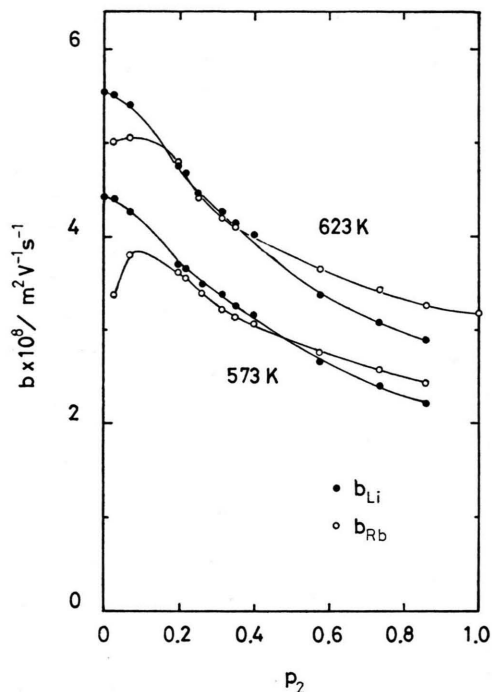


Fig. 5. Isotherms of internal cation mobilities in the system $(\text{Li-Rb})\text{NO}_3$.

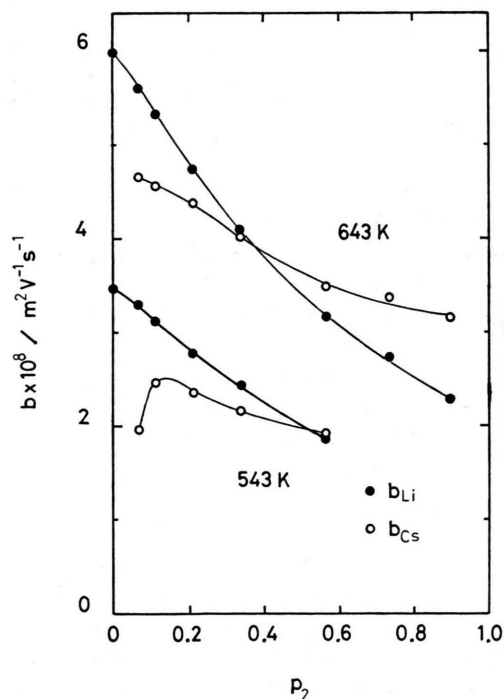


Fig. 6. Isotherms of internal cation mobilities in the system $(\text{Li-Cs})\text{NO}_3$.

of the latter. In fact, the self-diffusion coefficient of Li^+ is larger than that of M^+ in the mixtures so far studied in which the Chemla effect is found for the mobility [9].

In view of the fact that the well of the pair potential between Li^+ and Cl^- is very deep [26], that between Li^+ and NO_3^- is expected to be also deep. Therefore, although the small size and mass of Li^+ facilitate its movement along the "surface" of the nearest neighbouring NO_3^- , Li^+ cannot readily move away from the NO_3^- , unless another NO_3^- is present near it. In other words, an increase of the number density of NO_3^- will increase the probability that Li^+ moves away from one NO_3^- to another. The internal mobilities of Li^+ at 623 K in the nitrate mixtures so far studied are plotted against the molar volume in Figure 7. The internal mobility in the system $(\text{Li-K})\text{NO}_3$ is evaluated from the data on the external mobility ratio [9], the specific conductivity [27, 28] and the density [23]. That in the system $(\text{Li-Tl})\text{NO}_3$ is recalculated from the equivalent conductivity data given by Brillant [29]. Figure 7 shows that the internal mobility of Li^+ decreases monotonously with increasing molar volume irrespective of the kind of mixture except $(\text{Li-Ag})\text{NO}_3$ and $(\text{Li-Tl})\text{NO}_3$. As for $(\text{Li-Ag})\text{NO}_3$, the data taken from [11, 12] lie on the same curve while those from [13] deviate considerably. As for $(\text{Li-Tl})\text{NO}_3$, positive deviations occur at larger molar volumes, that is at high concentration of TlNO_3 . This would be caused by the extraordinarily high external mobility of NO_3^- in TlNO_3 compared with that in pure alkali nitrates. The external mobilities of NO_3^- at 693 K are evaluated to be 2.03, 2.03, 2.59, 2.35, and $3.37 \times 10^{-8} \text{ m}^2 \text{ V}^{-1} \text{ s}^{-1}$ in NaNO_3 , KNO_3 , RbNO_3 , CsNO_3 , and TlNO_3 , respectively, from the external transport numbers (NaNO_3 , KNO_3 [30], RbNO_3 [31], CsNO_3 , and TlNO_3 [31, 32]).

At any rate, it may be safely stated that at least in the systems $(\text{Li-Alk})\text{NO}_3$ (Alk = alkali metal) the internal mobility of Li^+ decreases with increasing molar volume, that is, with a decrease in the number density of NO_3^- , irrespective of the kind of mixture. However, from the data on the specific conductivity [33] and the molar volume [34] under high pressure, it follows that the isothermal equivalent conductivity of pure molten LiNO_3 decreases with decreasing molar volume, as shown in Figure 7. This may be because the motion of NO_3^- decreases due to

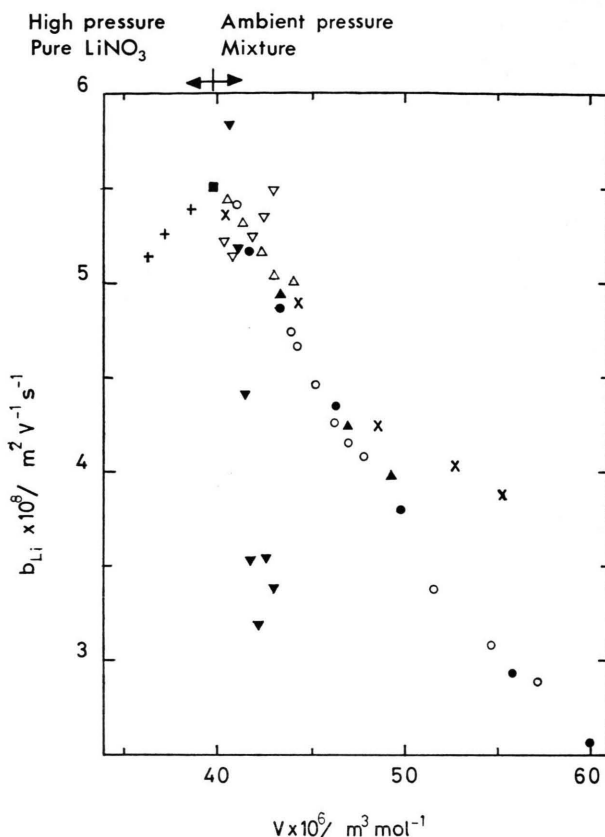


Fig. 7. Internal mobility of Li^+ at 623 K in pure LiNO_3 under high pressure (+ [33, 34]), ambient pressure (■ [23, 27]) and in mixtures $(\text{Li-M})\text{NO}_3$ at ambient pressure (\triangle M = Na [3], \blacktriangle K [9], \circ Rb, \bullet Cs, ∇ Ag [11, 12], \blacktriangledown Ag [13], \times Tl [14]).

the decrease of the free space with a further decrease in molar volume.

As for the internal mobility of the larger cation, the factor governing it is not so simple in appearance as that for Li^+ . At high LiNO_3 concentrations, particularly at low temperatures, b_2 decreases markedly with an increase of p_1 , as is seen from Figs. 5 and 6. The value of p_2 where the isotherms of b_2 have the maximum increases with decreasing temperature, and the molar volume of the corresponding mixtures seems to be nearly constant irrespective of temperature. This would indicate that there is a kind of critical volume for the free space large enough for a separating motion of the larger cation and NO_3^- . In this concept, the free space does not necessarily mean microscopic voids large enough to accommodate the ion wholly. Molecular dynamics studies show that many-event mechanisms involving

cooperative motions rather than jumping motions could well describe diffusion in molten salts [35].

Except the region very rich in Li^+ , b_2 increases with an increase of p_1 . From findings by molecular dynamics simulation [18], it is expected that, as p_1 is increased, the diffusive motion of NO_3^- and the large cation would be increasingly stimulated with attraction and repulsion, respectively, by the vigorous motion of Li^+ arising from its small size and mass. The stimulated diffusive motion would facilitate a separating motion of the large cation and NO_3^- , both because the well of the pair potential between them is not so deep as that between Li^+ and anion, and also because the probability that other NO_3^- ions are present very near the larger cation is high. Thus, while the large cation would affect the mobility of Li^+ in the mixture only through the molar volume change, Li^+ would act on that of the large cation in a somewhat more complicated way as stated above.

The Chemla effect therefore occurs as a consequence that b_1 decreases considerably with decreasing

p_1 , while b_2 increases moderately with decreasing p_2 .

As temperature increases, the volume of free space will increase. While this is favourable for the mobility of the large cation, the expansion of the free space, *per se*, will be unfavourable for that of Li^+ , as stated above. However, the decrease of the mobility caused by it would be masked with the overwhelming increase of the diffusive motion with rising temperature. Therefore, as temperature increases, b_1 increases somewhat moderately, while b_2 rises considerably. Consequently, the value of p_2 where b_1 and b_2 cross each other will decrease with increasing temperature.

In conclusion, the mobilities of both Li^+ and the large cation in the mixture could be explained consistently on the assumption that the dominant factors which rule these would be the pair potential between cation and anion and the ionic size as compared with the volume of free space. Although the mass of ions is really a factor ruling the diffusive motion and the mobility, it would be a minor factor in comparison with the above mentioned ones.

- [1] J. Périé, M. Chemla, and M. Gignoux, *Bull. Soc. Chim. Fr.* **1961**, 1249.
- [2] F. Lantelme and M. Chemla, *J. Chim. Phys.* **60**, 250 (1963).
- [3] C. Yang, R. Takagi, and I. Okada, to be published.
- [4] C. Moynihan and R. Laity, *J. Phys. Chem.* **68**, 3312 (1964).
- [5] M. Smirnov, K. Aleksandrov, and V. Khokhlov, *Electrochim. Acta* **22**, 543 (1977).
- [6] J. Périé and M. Chemla, *C. R. Acad. Sci.* **250**, 3986 (1960).
- [7] O. Metha, F. Lantelme, and M. Chemla, *Electrochim. Acta* **14**, 505 (1969).
- [8] Y. Yamamura and S. Suzuki, *J. Nucl. Sci. Technol.* **7**, 522 (1970).
- [9] F. Lantelme and M. Chemla, *Electrochim. Acta* **10**, 663 (1965).
- [10] V. Ljubimov and A. Lundén, *Z. Naturforsch.* **21a**, 1592 (1966).
- [11] M. Okada and K. Kawamura, *Denki Kagaku* **39**, 812 (1971).
- [12] K. Kawamura and M. Okada, *Electrochim. Acta* **16**, 1151 (1971).
- [13] J. Richter and E. Amkreutz, *Z. Naturforsch.* **27a**, 280 (1972).
- [14] K. Kawamura, I. Okada, and O. Odawara, *Z. Naturforsch.* **30a**, 69 (1975).
- [15] Commissariat à l'Énergie Atomique, *Brevet Français No. 1216418*. Inventor M. Chemla.
- [16] F. Lantelme and M. Chemla, *Bull. Soc. Chim. Fr.* **1963**, 2200.
- [17] F. Lantelme and M. Chemla, *Electrochim. Acta* **11**, 1023 (1966).
- [18] I. Okada, R. Takagi, and K. Kawamura, to be published.
- [19] I. Okada, *Z. Naturforsch.* **33a**, 498 (1978).
- [20] P. I. Protzenko, *Izvest. Sektora Fiz.-Khim. Anal. Inst. Obschei Neorg. Khim. Akad. Nauk SSSR* **26**, 173 (1955).
- [21] K. A. Bolshakov, B. I. Pokrovskii, and V. E. Plyushev, *Russ. J. Inorg. Chem.* **1961**, 1084.
- [22] B. de Nooijer, Thesis, Amsterdam 1965.
- [23] I. G. Murgulescu and S. Zuca, *Electrochim. Acta* **11**, 1383 (1966).
- [24] J. P. Hansen and I. R. McDonald, *Phys. Rev. A* **11**, 2111 (1975).
- [25] A. Klemm, *Z. Naturforsch.* **32a**, 927 (1977).
- [26] F. G. Fumi and M. P. Tosi, *J. Phys. Chem. Sol.* **25**, 31 (1964).
- [27] L. King and F. Duke, *J. Electrochem. Soc.* **111**, 712 (1964).
- [28] P. Dulieu, P. Aglave, and P. Claes, *Ann. Soc. Sci. Bruxelles* **86**, 109 (1972).
- [29] S. Brillant, Thesis, Strasbourg 1967.
- [30] F. Duke and B. Owens, *J. Electrochem. Soc.* **105**, 548 (1958).
- [31] D. Topor, *Rev. Roum. Chim.* **18**, 1311 (1973).
- [32] S. Forcheri and C. Monfrini, *J. Phys. Chem.* **67**, 1566 (1963).
- [33] G. Schlichthärle, K. Tödheide, and E. U. Franck, *Ber. Bunsenges. Phys. Chem.* **76**, 1168 (1972).
- [34] B. B. Owens, *J. Chem. Phys.* **44**, 3918 (1966).
- [35] L. V. Woodcock, "Advances in Molten Salts Vol. 3", ed. by J. Braunstein et al., Plenum, New York 1975, p. 1.